*Middle Tennessee State University* DE-FG05-86ER40293-7

# NUCLEAR STRUCTURE STUDIES *via* NEUTRON INTERACTIONS

Progress Report
1 July 1992 – 30 June 1993

Robert F. Carlton
Principal Investigator
Dept. of Chemistry & Physics

Dr. Myra Norman, Director
Sponsored Programs

Middle Tennessee State University
Murfreesboro, Tennessee 37132
March 1993

Prepared for
THE U.S. DEPARTMENT OF ENERGY
Under Contract No. DE-FG05-86ER40293

## ABSTRACT

Comparison has been made between the empirical integrated strengths and external R-functions and the predictions of a dispersive optical model for the n – $^{208}$Pb system, for partial waves through $f_{7/2}$. Parameters of a constant geometry model give a fair representation of the experimental results. A hint of the need for a parity dependence in one of the model parameters is seen in the two data and in the total cross section in the low-energy region. Other research performed consisted of: (1) refinement of the resonance analysis of the n – $^{208}$Pb system, resulting in more definitive $J^{\pi}$ assignments and external R-functions consistent over the neutron energy range [80 – 1760 keV]; (2) background correction and processing of n – $^{88}$Sr differential scattering cross section data for use with total cross section data for R-matrix analysis ; (3) measurment of the n – $^{90}$Zr differential scattering cross section at the 200-m flight path of the ORELA

## I. Introduction

During the current reporting period we have completed the analysis of the total cross section data for the $^{208}$Pb target nucleus to obtain a set of resonance parameters and external R-functions from which we can obtain scattering functions for each of the partial waves participating in the interaction. We are currently in the process of applying the dispersive optical model analysis (DOMA) to the elastic scattering results.

The investigation has covered the energy range $E_n$ = 80-1760 keV. Partial waves through $f_{7/2}$ have been observed and the associated R-functions and strength functions have been obtained. Because the data above 1 MeV manifest some overlap and thus strong level-level interference, internal consistency of the data set, among resonance and non-resonance parameters over the entire energy range, has been a criterion used to arbitrate the ambiguities in $J^\pi$ values deduced solely on the basis of resonance shapes.

We had previously obtained resonance parameters and tentative $J^\pi$ assignments over this energy range, but found that the R-external functions required by the low-energy region were inconsistent with those required above 1200 keV. This refinement resulted in the removal of some of the ambiguity in the $J^\pi$ assignments and a clarification of the trends of the R-external functions over the entire energy range.

Since the analysis of the $^{208}$Pb data presents fewer complications than for $^{48}$Ca, we have decided to complete the former analysis first. Attempt will be made to complete the $^{48}$Ca analysis during the next period.

One month in the summer was spent at ORNL, performing differential scattering measurements on $^{90}$Zr + n and processing the $^{88}$Sr + n differential scattering data for use in the R-matrix resonance analysis of total cross section data. These isotopes will provide the focus of the next analysis in pursuit of the goals of the current contract.

## II. Dispersive Optical Model

Traditionally the phenomenological optical model has served to provide a global description of an extensive data set consisting of differential elastic scattering, polarization and total cross section data for many target nuclei. The model has been characterized by energy independent geometries and energy dependent potential depths. One characteristic, however, has been the consistent failure to adequately predict the experimental cross sections at energies below approximately 10 MeV without introducing energy dependent geometries which were different for different nuclei. Since

this is ostensively connected with nuclear structure effects, Mahaux and Ngô[1] have introduced a dispersive correction to the optical potential which is determined by surface interactions. This has the effect of modulating the real potential in the vicinity of the Fermi energy and thus accounting in a physical way for the energy dependence of the potential geometry required by the simple global optical analyses.

Application of the dispersive optical model approach (DOMA) to the n – $^{40}$Ca[2] and n - $^{208}$Pb[3] systems has resulted in a unified description of the interaction in the bound, or shell model, region as well as the unbound region all with a single potential. One can obtain the dispersive correction from a knowledge of the imaginary potential through the dispersion relation,

$$\Delta\mathcal{V}(E;r) = \frac{\mathrm{P}}{\pi}\int_{-\infty}^{\infty} \frac{W(E';r)}{E'-E}\,dE', \qquad (1)$$

where P represents the principal value integral and $W$ is the imaginary potential. It is this correction which provides the modulation of the real potential and which obviates the need for energy dependence in the geometry. The real part of the full potential is then given by

$$\mathcal{V}(E\,;\,r) = V_{HF}(E\,;\,r) + \Delta\mathcal{V}(E\,;\,r), \qquad (2)$$

where $V_{HF}$ is the Hartree-Fock potential, having a Woods-Saxon form and an exponential energy dependence of the form $V_{HF}(\mathrm{E}) = \mathrm{V}_{HF}(0)\exp(-\alpha\mathrm{E})$. The geometry of this part of the potential is taken to be energy independent.

One thus must have a knowledge of the imaginary potential, $W$, which is written as a sum of surface and volume contributions,

$$W(r\,;\,E) = W_v(r\,;\,E) + W_s(r\,;\,E), \qquad (3)$$

with the volume part having a Woods-Saxon shape and the surface part that of a radial derivative of a Woods-Saxon form factor. One can then obtain volume and surface contributions to the dispersive correction, once the functional form of $W$ is known. The depth of the potential is parametrized[4] in terms of the volume integrals per nucleon of the total and volume imaginary potentials, $\mathrm{J}_W$, and $\mathrm{J}_{W_v}$,

$$J_{W,v}(r\ ;\ E) = J_W \left\{ \frac{\varepsilon^2}{\varepsilon^2 + \varepsilon_{\rho,v}^2} \right\}. \tag{4}$$

That of the surface imaginary component has been parametrized in at least two ways; by the difference between two of these Brown-Rho (BR) forms, known as the BR – BR parametrization,

$$J_s(r\ ;\ E) = J_W \left\{ \frac{\varepsilon^2}{\varepsilon^2 + \rho^2} - \frac{\varepsilon^2}{\varepsilon^2 + \varepsilon_v^2} \right\}, \tag{5}$$

and by the BR – JM parametrization where the subtracted term, due to Jeukeene & Mahaux[5], is represented as,

$$J_{JM}(r\ ;\ E) = J_{JM} \left\{ \frac{\varepsilon^4}{\varepsilon^4 + \mu^4} \right\}. \tag{6}$$

The energy, $\varepsilon$, is that relative to the Fermi energy, $E_F$, *i.e.*, $\varepsilon = E\text{-}E_F$. The procedure usually followed is to perform a least squares fit of all available cross section data to deduce the parameters of the model. Due to the number of parameters in the model, this requires an extensive dataset covering a large energy range. The present study does not fit that criterion so we have taken the approach of investigating the predictions of the model using the parameters deduced from the more extensive datasets. Failure of the model to explain the features of the current study, may be attributed to more microscopic effects than can be incorporated in a global model. Or, it may be possible to use this detailed information to further refine the model. We currently have only considered the first of these two possibilities, and have adopted the BR – BR parameterization for the surface imaginary potential. We plan to explore the other possibility and the JM parametrization in the next period.

## III. Dispersive Optical Model Applied to n – $^{208}$Pb.

Much experimental data is available on neutron – $^{208}$Pb elastic scattering, including differential, polarization and total cross sections. More recently Johnson, *et. al.*[6] analyzed the available experimental data for n – $^{208}$Pb in the framework of the

dispersive optical model (DOMA) and found that the data above 10 MeV could be fit satisfactorily with the radius, $r_s$, and diffuseness, $a_s$, of the surface imaginary potential independent of energy. In addition, predictions of the single particle energies in the range $[-20\ \text{MeV} < E < 0\ \text{MeV}]$ were in good agreement with the observed values. However, the data between 0 and 10 MeV were not properly described by this constant geometry model. Similar low-energy problems in the total cross section have been seen in studies of $n - {}^{40}Ca$[2] and $n - {}^{40}Ar$[7]. Juekenne, *et. al.*[8]considered several modifications of the work of Johnson[6] in an attempt to improve the fits of the low-energy scattering and total cross section data. The best overall fits to the low-energy data, which preserved the quality of the fits to the higher energy data, were obtained for a model which incorporated a simple angular momentum dependence and an energy dependent diffuseness, $a_s$, for the surface component of the imaginary potential. Since the present experimental work is the only one capable of providing a description of the energy-averaged scattering function for <u>*each*</u> contributing partial wave in the low energy region, it is worth considering the degree to which the energy-averaged scattering functions, deduced at low energies (80 – 1760 keV), are reproduced by the parameters of the dispersive optical model, deduced from high energy data and the information on states in the bound region. We have thus taken the parameters for $^{208}$Pb, deduced in the framework of the DOMA with the simplest assumptions, *i.e.,* energy independent geometric parameters and angular momentum-independent well depths .

### A. Parametrization of the Model.

The quantity, $\varepsilon$, in the latest work[9]on the $n - {}^{208}Pb$ system is the energy relative to the threshold energy, $E_o \equiv < E_p >$, which is taken to be the centroid of the particle valence shells and for $^{208}$Pb is ,

$$E_o = \frac{1}{7} \sum_{n\ell j \in p} E_{n\ell j} \tag{7}$$

in the region above the Fermi energy, $E_F$. This latter energy is identified with the average of this and a similar expression for the centroid of the hole valence shells, below the Fermi energy. The earlier BR parametrizations have the disadvantage that the imaginary potential does not vanish for energies between the Fermi energy and that of the $2g_{9/2}$ state, *i.e.,* for energies lower than the ground state of $^{208}$Pb and thus are unphysical. Following Mahaux and Sartor[10], we have parametrized $W$ so that it

vanishes for energies located between $E_F$ and $< E_p >$.

Since all the parameters needed for the BR – BR parametrization of the $^{208}$Pb potential are not available in the literature, namely the parameter $\epsilon_v$, and since we find this parameter to have little influence upon the energy-averaged scattering functions in the low energy region, we have used a reasonable value for $\epsilon_v$, together with those listed below[9]:

$V_H = 46.4$ Mev; $V_{so} = 5.75$ Mev;
$r_H = 1.225$ fm; $r_{so} = 1.105$ fm;
$a_H = 0.70$ fm; $a_{so} = 0.50$ fm;
$\alpha_H = -0.31$;

$\rho = 6.02$ MeV; $\epsilon_v = 36.0$ MeV;
$r_W = 1.27$ fm; $r_v = 1.27$ fm;
$a_W = 0.70$ fm; $a_v = 0.70$ fm;
$E_F = 5.57$ MeV; $E_o = 2.17$ MeV;
$J_W = 63.1$ MeV.

The influence of the depth of the Hartree-Fock component of the real potential upon the placement of the particle and hole states in the valence shells has been explored and from Fig. 1 it can be seen that the value of the well depth is narrowly restricted to a range between 46.4 MeV and 47.0 MeV, for the set of parameters given above. The symbol J(v) in Fig. 1 represents the volume integral of the imaginary component of the potential. The solid line in the figure corresponds to the experimental values of the binding energies of the indicated valence states.

The excellent agreement between the experimental and predicted binding energies is seen in Fig. 2, where only the states for which the current data yields information in the unbound region are included. The values on the right correspond to the full potential of the DOMA, including the surface contributions to the real potential, namely, $\mathcal{V} = \mathcal{V}_v + \Delta\mathcal{V}_s$.

Similar investigations of the influence of the volume integral, $J_W$, on the positions of the valence shells have similarly corroborated the value of this parameter of the model. Since, as noted earlier, published results for DOMA of the n – $^{208}$Pb interaction do not include the BR – BR parametrization of the surface imaginary potential, we have

investigated a range of values consistent with those used in studies of other systems where this parametrization was used. Values for the parameter $\epsilon_v$ have thus been varied, from the value indicated above, by a factor of two to see the influence of the parameter on the model predictions. Based on the predicted integrated strengths of the individual partial waves, we find that this variation results in at most a 10% difference in the model predictions for this quantity. This confirms the insensitivity of the model to this parameter for predictions pertaining to the scattering function at low energies. Further investigation in the next period will assure that the parameters used will also be consistent with predictions at higher energies.

### B. Relating the Dispersive Optical Model to the R-matrix Results.

The primary motivation of the high resolution measurements was to resolve resonances in the neutron total cross section for energies below the inelastic threshold at 2.6 MeV. The R-matrix provides us with detailed descriptions of the neutron scattering functions for the $s_{1/2}$— $f_{7/2}$ partial waves for the energy domain [$E_\ell$, $E_u$] from $E_\ell$= *0.0* to $E_u$= *1.765* MeV. Our approach is to compare the energy averages of those scattering functions to the optical model predictions for the same partial waves.

Since only the entrance neutron channel is important for the domain [$E_\ell$, $E_u$], the R-matrix reduces to an R-function where, for the total angular momentum $j = \ell \pm \frac{1}{2}$, the scattering function reads

$$S_{\ell j}(E) = e^{-2\phi_\ell(E)} \cdot \frac{1 + iP_\ell(E)\, R_{\ell j}(E)}{1 - iP_\ell(E)\, R_{\ell j}(E)} , \qquad (8)$$

where $P_\ell(E)$ and $\phi_\ell(E)$ are the penetrability and the hard-sphere phase shift evaluated at the channel radius $a_c$. The value of $a_c$ is arbitrary, except that it should be near the nuclear radius. Once chosen, however, it should be used in both the data analysis and optical model. We have used a value of 8.59 fm. The R-function, $R_{\ell j}(E)$, is a sum over the n – resonances with quantum numbers $\ell$ and $j$ that are observed within the domain [$E_\ell$, $E_u$], plus an external R-function which accounts for the influence of levels outside the domain, and is expressed as

$$R_{\ell j}(E) = \sum_{\lambda=1}^{n} \frac{\gamma^2_{\ell j\lambda}}{E_{\ell j\lambda} - E} + R^{ext}_{\ell j}(E) , \qquad (9)$$

where $E_{\ell j\lambda}$ and $\gamma^2_{\ell j\lambda}$ are the energy and reduced width of the $\lambda$th level.

From eqn. (10) we can see that the empirical scattering function has a very detailed energy dependence. To compare with the model predictions we first average over energy. Good agreement between model and experiment requires that the model scattering function be approximately equal to the smoothed experimental average;

$$S^{OM}_{\ell j}(E) = < S_{\ell j}(E) > . \tag{10}$$

Expanding the model scattering function (using the same channel radius) in the same form as for the experimental scattering function,

$$S^{OM}_{\ell j}(E) = e^{-2\phi_\ell(E)} \cdot \frac{1 + iP_\ell(E)\, \Re^{OM}_{\ell j}(E)}{1 - iP_\ell(E)\, \Re^{OM}_{\ell j}(E)} , \tag{11}$$

with

$$\Re^{OM}_{\ell j}(E) = R^{OM}_{\ell j}(E) + i\,\pi \cdot s^{OM}_{\ell j}(E) , \tag{12}$$

we can use the following simple prescription[11] for comparing the model functions to the averaged empirical functions for a given $\ell$J:

$$\sum_{\lambda=1}^{k} \gamma^2_{\ell j\lambda} \simeq \int_{E_\ell}^{E_u} s^{OM}_{\ell j}(E')\, dE' , \tag{13}$$

and

$$R^{ext}_{\ell j}(E) \simeq R^{OM}_{\ell j}(E) - P \int_{E_\ell}^{E_u} \frac{s^{OM}_{\ell j}(E')\, dE'}{(E' - E)} , \tag{14}$$

where P denotes the principal value integral.

## IV. Results.

### 1. Integrated Strength

Results for the first of these equations, for the even-parity states, are presented in Fig. 3. The "staircases" represent cumulative sums of reduced widths up to neutron energy E. Each riser is a reduced width, $\gamma^2_{\ell j\lambda}$, and each tread is the spacing between adjacent levels. The curves represent the predictions of the model. Model predictions are seen to underestimate the strength of even-parity states, accounting for approximately 60% of the observed strength in the analyzed region, for each partial wave. While the model cannot account for the absence of $s_{1/2}$ strength below 500 keV, it gives a reasonable representation by the time the energy reaches 2 MeV. The absolute strengths of the even parity states are very comparable, reflecting the fact that all these states are rather closely spaced and are just bound.

Results for the odd-parity states are seen in Fig. 4. Here the results are not as good as for the even-parity states. The model is seen to overestimate the strength for all but the $f_{5/2}$ states, by as much as a factor of 2.5. The anomaly associated with the $f_{5/2}$ state may be heightened by possible missassignments between the $f_{5/2}$ and $f_{7/2}$ states, but still, the underestimate would likely persist even if resonances of uncertain $J^\pi$ were apportioned between the two $\ell = 3$ states on the basis of spin-statistical weighting. The shape of the staircase for the $f_{5/2}$ is characteristic of an excess number of levels having been assigned to this spin state. The Dyson – Mehta $\Delta_3$ statistic may prove useful in reassigning the weak levels for $\ell = 3$ between the two j-values.

The over- and under-estimation for the different parity states suggests that a parity dependence of at least one of the model parameters could account for all observed strengths. Other investigations[6,8] of a possible parity dependence has shown that at least a simple parity dependence does not degrade the model predictions at higher energies, and in fact improves the description of the total cross section in the energy region just above that of the present investigation.

**2. External R-functions**

In Fig. 5 we present the model predictions of the second of the two equations above for all the partial waves observed in the energy domain [$E_\ell$ , $E_u$]. For each parity the the symbols give the parametrization of the external R-functions necessary to reproduce the resonance-potential and resonance-resonance interference patterns. The open circles represent the lower j-value and the open triangles the upper j-value for each parity. The smooth curves give the model predictions, with the solid and dashed curves representing the lower and upper j-values, respectively. The relative uncertainties of the empirical R-functions have not yet been established but are approximately $0.05 - 0.10$.

It is found in the case of the R-functions that the model under predicts all partial waves except the $p$-waves, which are overestimated. This is similar to the results for the integrated strengths found above, giving additional support to the suggestion that minor adjustment of the model, corresponding to a parity dependence, could improve the overall representation of the data. The shapes of the empirical and the model representations are inconsistent for both the $d_{3/2}$ and the $f_{7/2}$. It is not clear at this point whether a different parametrization of the potential will correct this or if the shape is incorrect for the empirical case due to the fact that little information is available below 600 keV to constrain the low energy portion. This will be investigated.

**3. Total Cross Section ($0 < E_n < 20$ MeV):**

The most notable failure of the dispersive optical model, as applied to the n–$^{40}$Ar[7] and n–$^{40}$Ca[2] systems has been in fitting the total cross section for $2 < E_n < 11$ MeV. A similar inadequacy was obtained for the n – $^{208}$Pb system[6] in the constant geometry models. For the latter nuclide, the introduction of an energy dependence in the diffuseness of the surface imaginary potential, $a_s$, together with a simple parity dependence has been shown to improve the prediction of the total cross section in this energy region. We present in Fig. 6 the predictions of the DOMA for the BR – BR parametrization with the parameters given above. The open circles represent energy-averaged total cross section data and the curve gives the model predictions. The fit in the minima at approximately 2 and 8 MeV and the peak in the cross section near 4 MeV show a need for some improvement. This will also be investigated with the alternate parametrization planned in the next period.

## V. Conclusions

Given the average nature of the optical model and its ability to provide a global description of extensive data for many nuclei, it is notable that the agreement of the model predictions with the detailed information from the present work is as good as it is. Almost all predictions of the energy averaged quantities agree with the empirical values within the magnitude of the quantity being modeled.

All of the comparisons seen in this investigation hint that a parity dependence in the parametrization of the dispersive optical model could result in an improvement in agreement with the data measured in the low energy region. If this could be achieved without affecting the agreement of model predictions for other data, then the global description achieved would be complete, describing not only information on bound and unbound states, but also detailed information in the low energy, resolved resonance region.

There are several means of introducing a parity dependence in the potential. The question to be explored will be the manner that will least impact the predictions of the model at energies outside the domain of this investigation. One possibility is the choice of the threshold energy, $E_o$. This is the most likely candidate since, at large energies, it becomes less important in comparison to the neutron energy. In addition, this approach could be justified since the energy at which one should expect interactions, for a given $n\ell j$, must exceed the energy of the first available state in the valence shell. Choosing $E_o$ to be $E_p$ rather than $E_{<p>}$ is thus more physically meaningful and will allow for different results for different parities. The question will be that of the magnitude of the effect this parameter will have upon the predicted quantities.

Other possible approaches to consider include (1) variation of the volume integral of the total imaginary potential, $J_W$, for each parity and (2) whether parametrizations of the surface imaginary potential that have been used for high energy data and for other target nuclei would account for the observed strengths without the need for a parity dependence. The BR – JM parametrization of the surface imaginary potential, with and without an energy dependent surface diffuseness will also be explored in the next period.

## VI. Projections

In addition to the additional investigations mentioned above, the interpretation of similar data for the n – $^{48}$Ca system will be explored to see if similar agreement can be obtained for non-closed-shell nuclei, after appropriate corrections for differences in the isovector potential corresponding to the different asymmetry coefficients involved. Finally, if time permits, we hope to automate this manual investigative process by integrating all the codes associated with this particular model investigation into a single code which is least squares driven, thus permitting more extensive and quantitative studies, and to integrate it with the graphical user interface of the X-window system.

Since the reanalysis of the $^{208}$Pb resonances was necessary to obtain scattering functions suitable for comparison to the DOMA, and since the successful model interpretation (by a novice) should be less prone to mistake for the $^{208}$Pb nuclide, this took precedence over the completion of the interpretation of the $^{48}$Ca results. Every effort will be made to complete this comparison in the next period.

Since we have not yet been able to obtain new total and scattering cross section data for $^{40}$Ca, any analysis in the next period will focus on either the Sr or Zr data already available. Thus there will likely be some rearrangement in the proposed schedule of activities for the 92-95 period, but no new directions are anticipated, unless unexpected opportunities for involvement with the efforts of the ORELA collaborators is warranted.

## Figure Captions

1. Investigation of the dependence of the valence binding energies upon the depth of a Hartree-Fock potential well. The legend gives the well depth, $V_{HF}$, and the title gives the values of the other parameters of the dispersive optical model used[9].
2. Predicted single particle energies in $^{208}$Pb using the parameters of the DOMA given in section III. A. Only those states corresponding to partial waves deduced in the R-matrix analysis are included. The level positions on the right hand side are the predictions based on the full real potential, including dispersive corrections from both volume and surface imaginary contributions.
3. Empirical results and model predictions for the integrated strength for those even parity states observed in the analysis. The staircase plots represent the empirical results and the curves are the model predictions.
4. Empirical and model predictions of results similar to those of Fig 3. for odd parity states.
5. External R-functions deduced from the R-matrix analysis for each partial wave through $f_{7/2}$. In each cell the open circles correspond to the parametrization necessary to provide the proper asymmetry in the total cross section for resonances of the lowest J-value for a given parity state. The open triangles correspond to that of the higher J-value member. The solid and dashed curves correspond, respectively to the model predictions for the lower- and upper- J-value members of each parity. Error bars are not given, but are not greater than 0.1 and not less than 0.05.
6. The total cross section for the n + $^{208}$Pb reaction over the energy range $0 < E_n < 20$ MeV. The circles represent averages of the measured cross section and the smooth curve corresponds to the model predictions using the parameters discussed in section III. A. The open circles below 3 MeV result from an average of the ORELA cross section data used in the resonances analysis. Those above 4 MeV are from the same source as Fig. 7 in Reference 6.

## References

[1] C. Mahaux, and H. Ngô, Nucl. Phys. **A378,** 205 (1982).

[2] C. H. Johnson, and C. Mahaux, Phys. Rev. **C 38,** 2589 (1988).

[3] J. P. Jeukeene, C. H. Johnson, and C. Mahaux, Phys. Rev. **C 38,** 2573 (1988).

[4] G. E. Brown, and M. Rho, Nucl. Phys. **A372,** 397 (1981).

[5] J. P. Jeukeene and C. Mahaux, Nucl. Phys. **A394,** 445 (1983).

[6] C. H. Johnson, D. J. Horen, and C. Mahaux, Phys. Rev. **C 36,** 2252 (1987).

[7] C. H. Johnson, R. F. Carlton, and R. R. Winters, Phys. Rev. **C 44,** 657 (1991).

[8] J. P. Jeukeene, C. H. Johnson, and C. Mahaux, Phys. Rev. **C 38,** 2573 (1988).

[9] C. Mahaux, and R. Sartor, in *Advances in Nuclear Physics* (J. W. Negele, and E. Vogt, eds.), Vol. 20, Plenum Press, New York (1991), p. 1.

[10] C. Mahaux, and R. Sartor, Nucl. Phys. **A503,** 525 (1989).

[11] C. H. Johnson, N. M. Larson, C. Mahaux, and R. R. Winters, Phys. Rev. **C 31,** 1563 (1984).

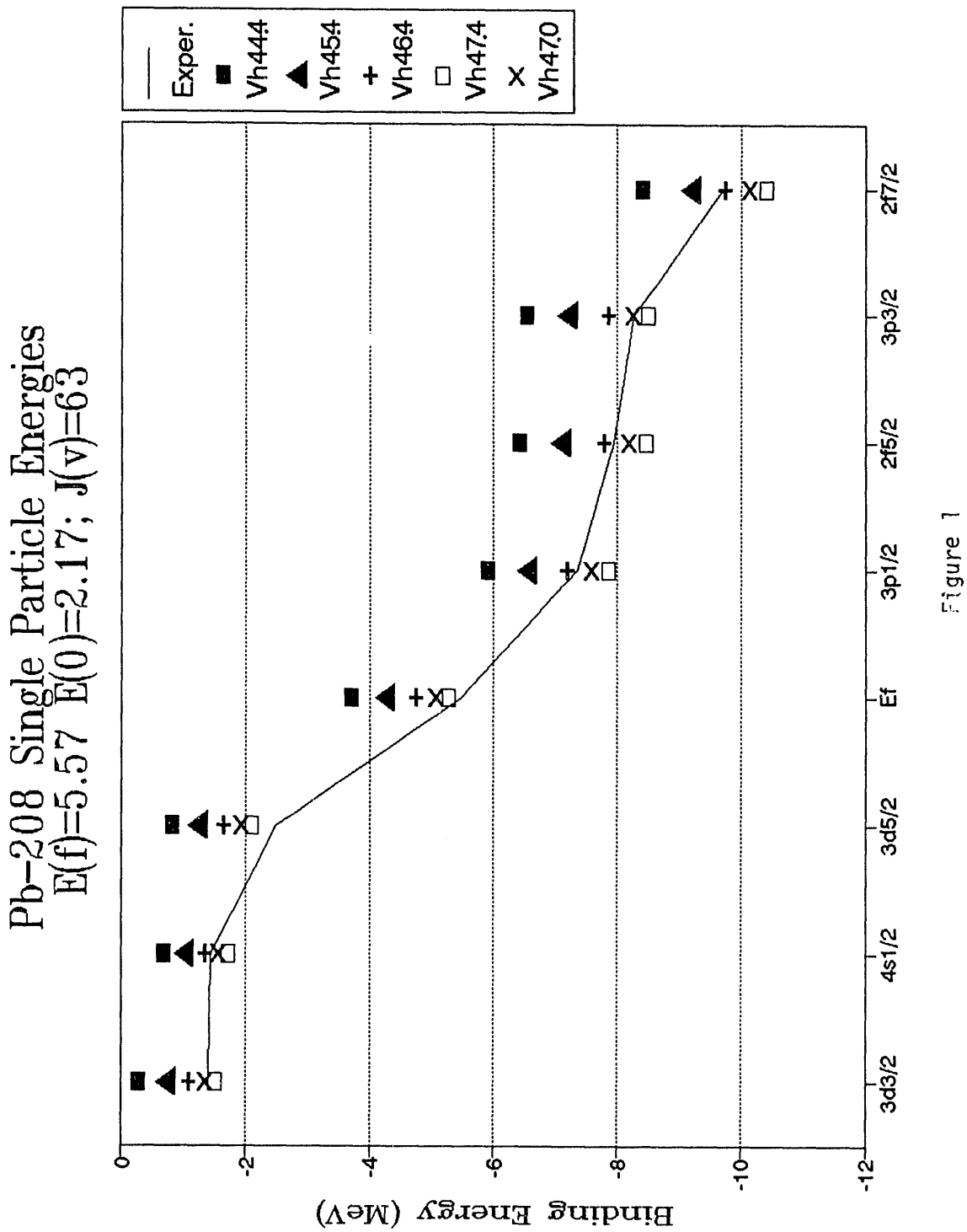
Pb-208 Single Particle Energies
E(f)=5.57 E(0)=2.17; J(v)=63
Exper.
Vh444
Vh454
Vh464
Vh474
Vh470
Binding Energy (MeV)
0
-2
-4
-6
-8
-10
-12
3d3/2
4s1/2
3d5/2
Ef
3p1/2
2f5/2
3p3/2
2f7/2

Figure 1

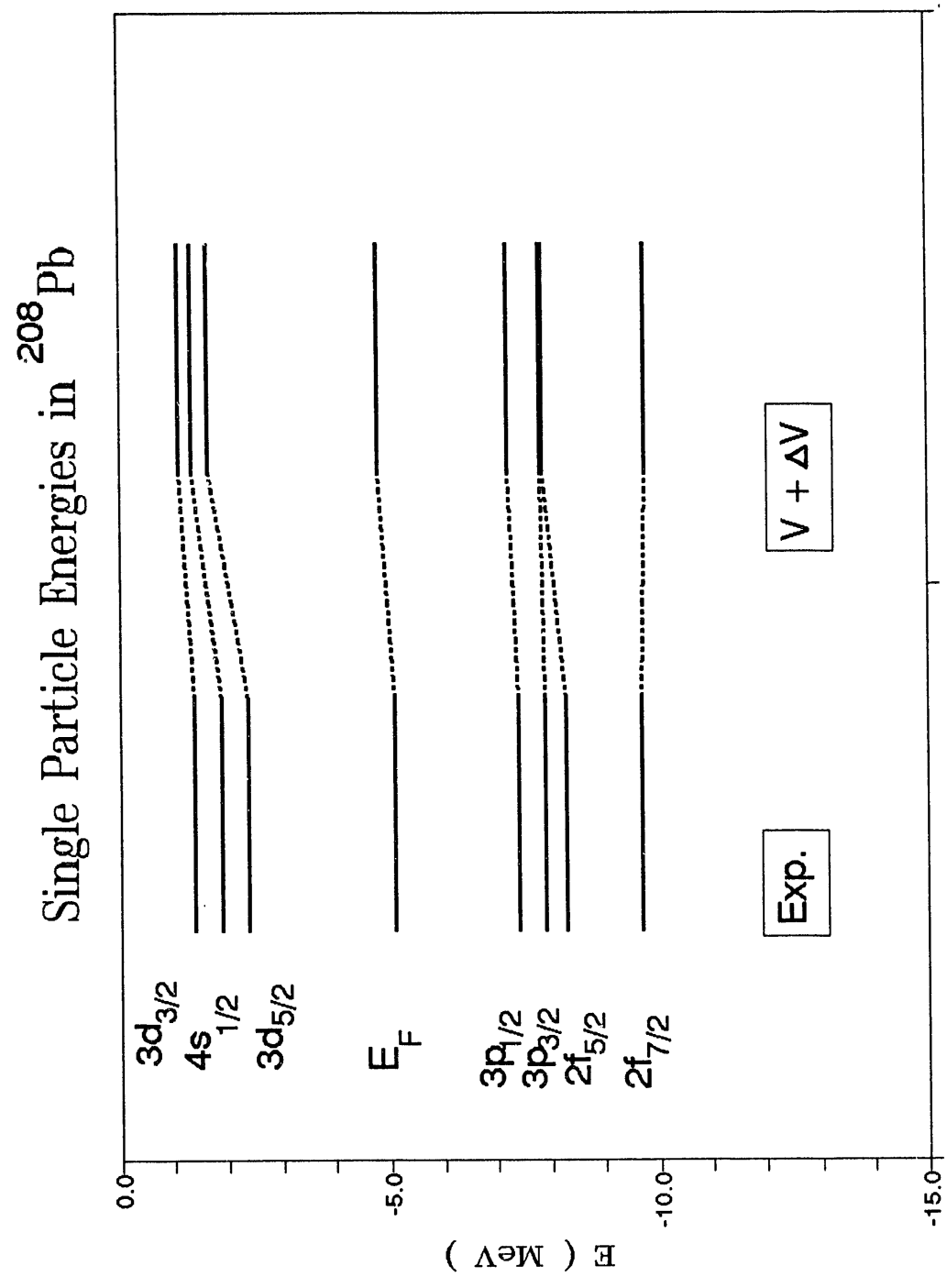
Single Particle Energies in $^{208}$Pb
E ( MeV )
0.0
-5.0
-10.0
-15.0
$3d_{3/2}$
$4s_{1/2}$
$3d_{5/2}$
$E_F$
$3p_{1/2}$
$3p_{3/2}$
$2f_{5/2}$
$2f_{7/2}$
Exp.
V + ΔV

Figure 2

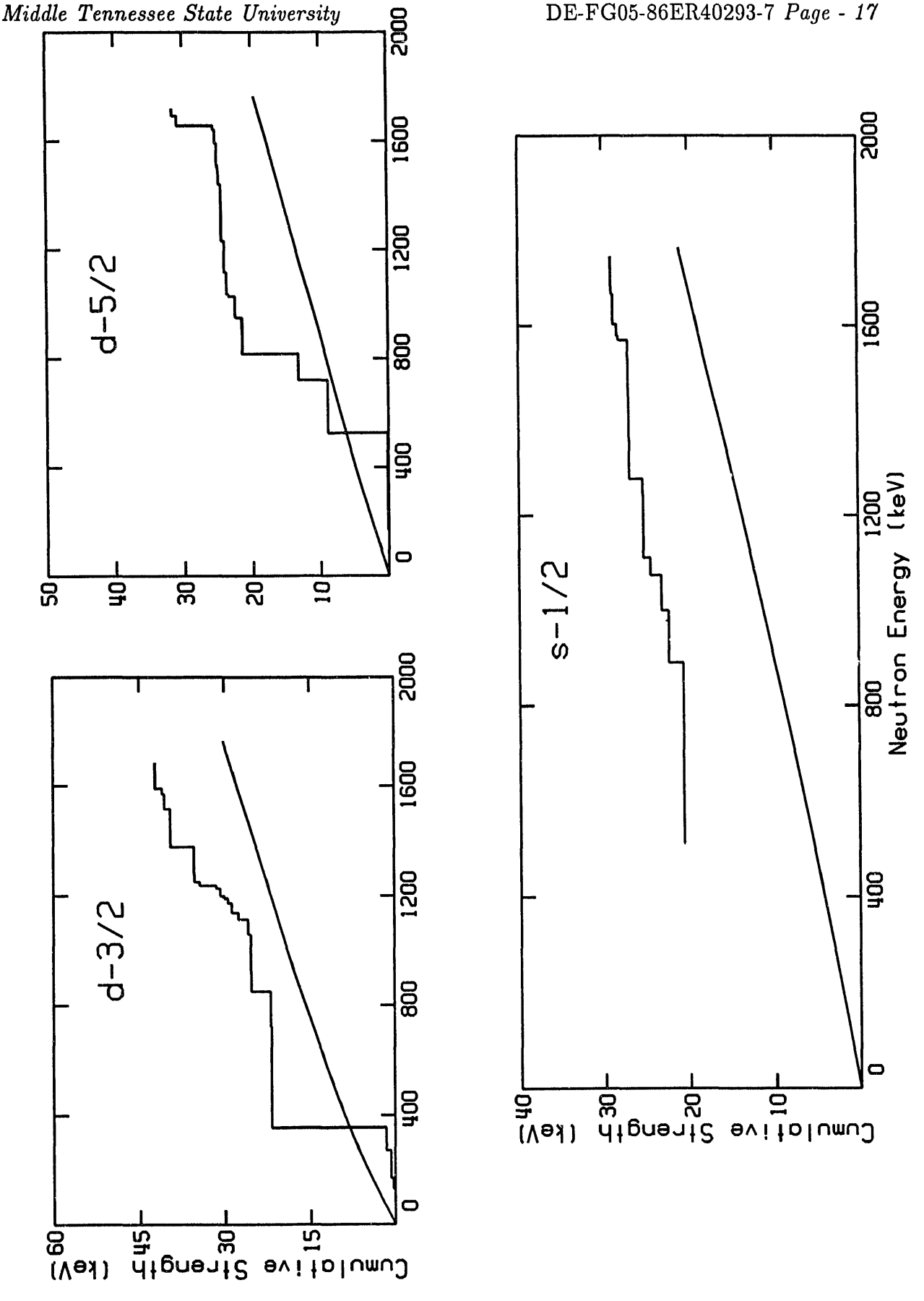
d-5/2
d-3/2
s-1/2
Cumulative Strength (keV)
Neutron Energy (keV)
0
400
800
1200
1600
2000
10
20
30
40
50
15
45
60

Figure 3

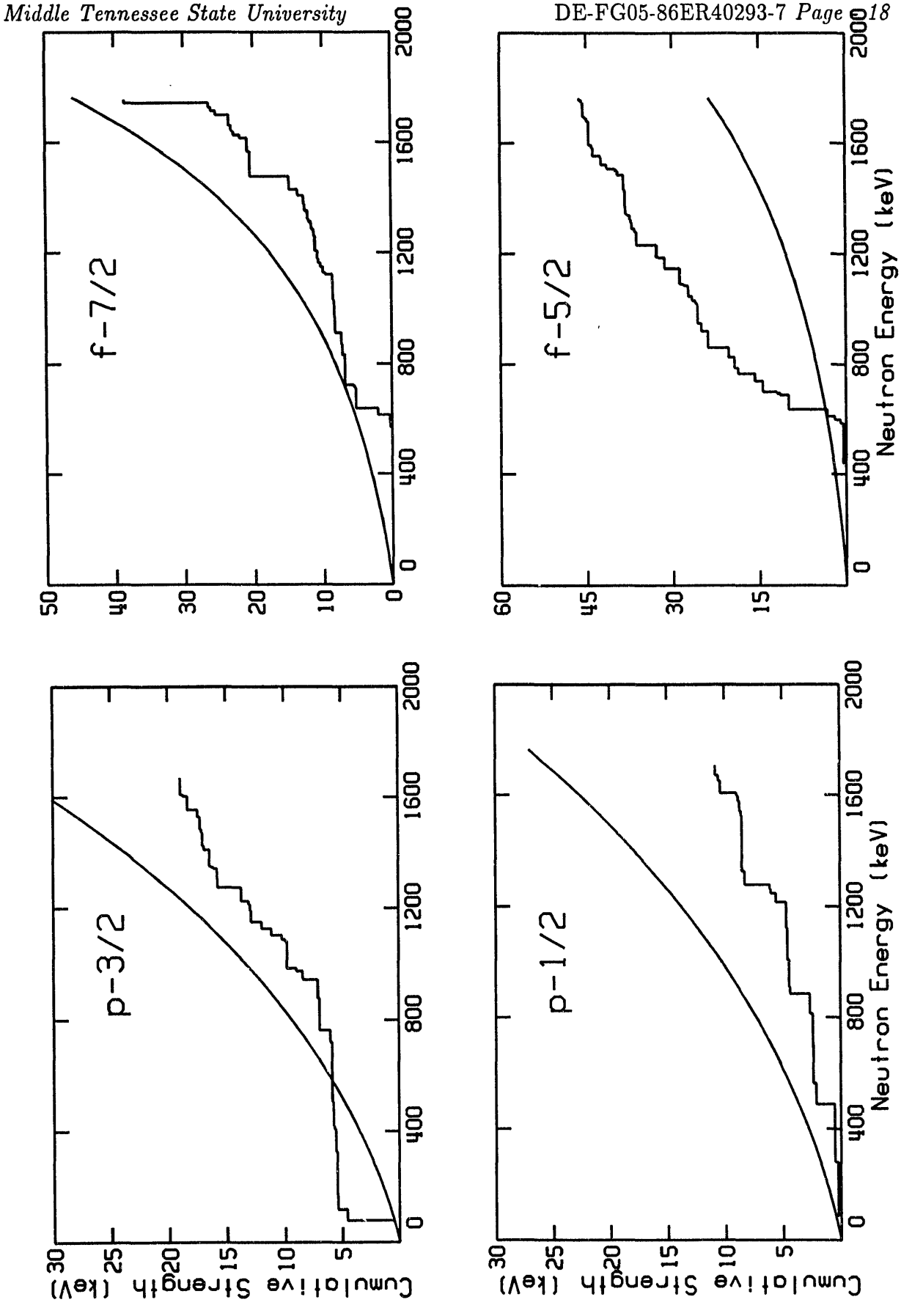
f-7/2
f-5/2
p-3/2
p-1/2
Cumulative Strength (keV)
Neutron Energy (keV)
0
400
800
1200
1600
2000
10
20
30
40
50
15
30
45
60
5
10
15
20
25
30

Figure 4

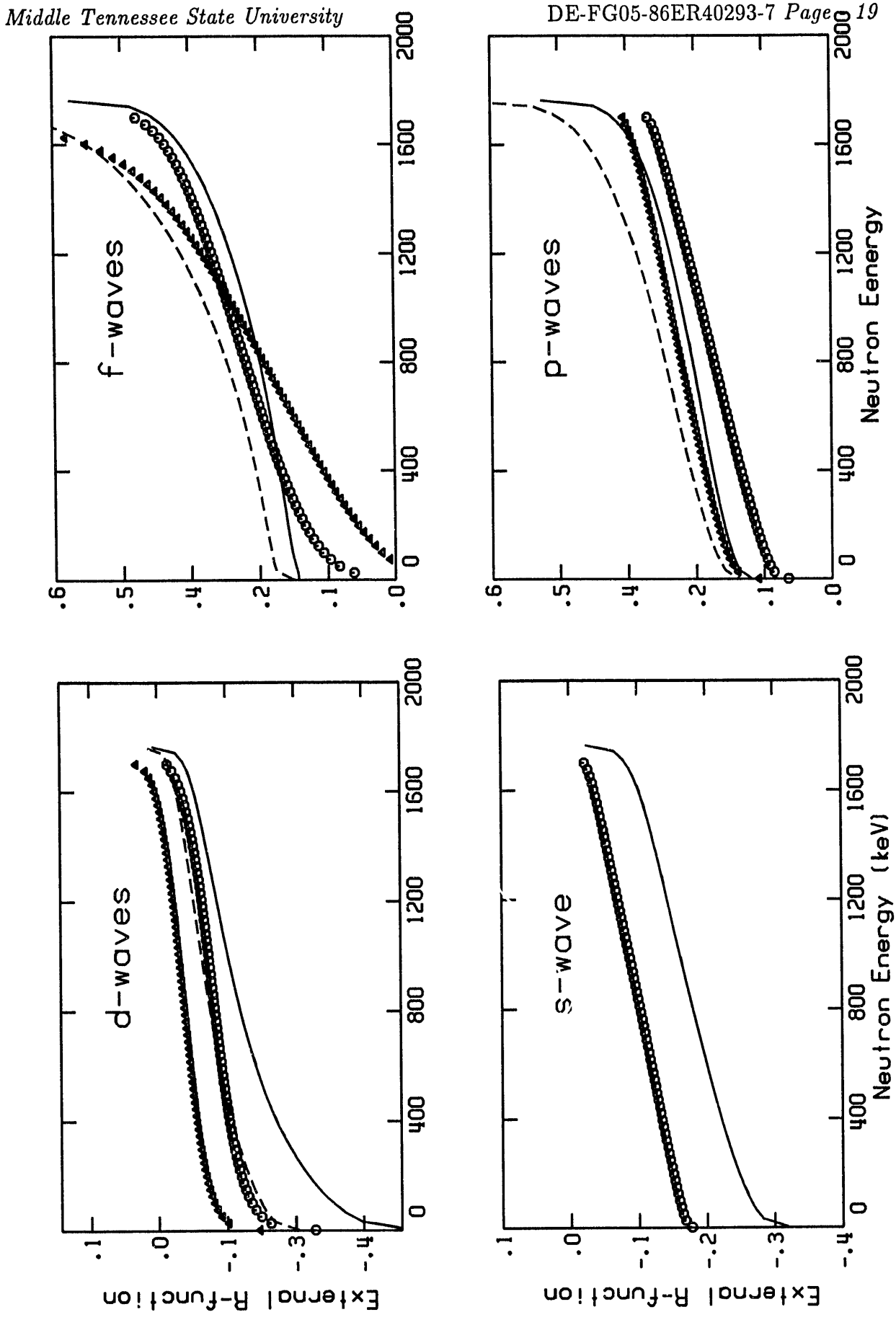
f-waves
p-waves
d-waves
s-wave
External R-function
Neutron Energy (keV)

Figure 5

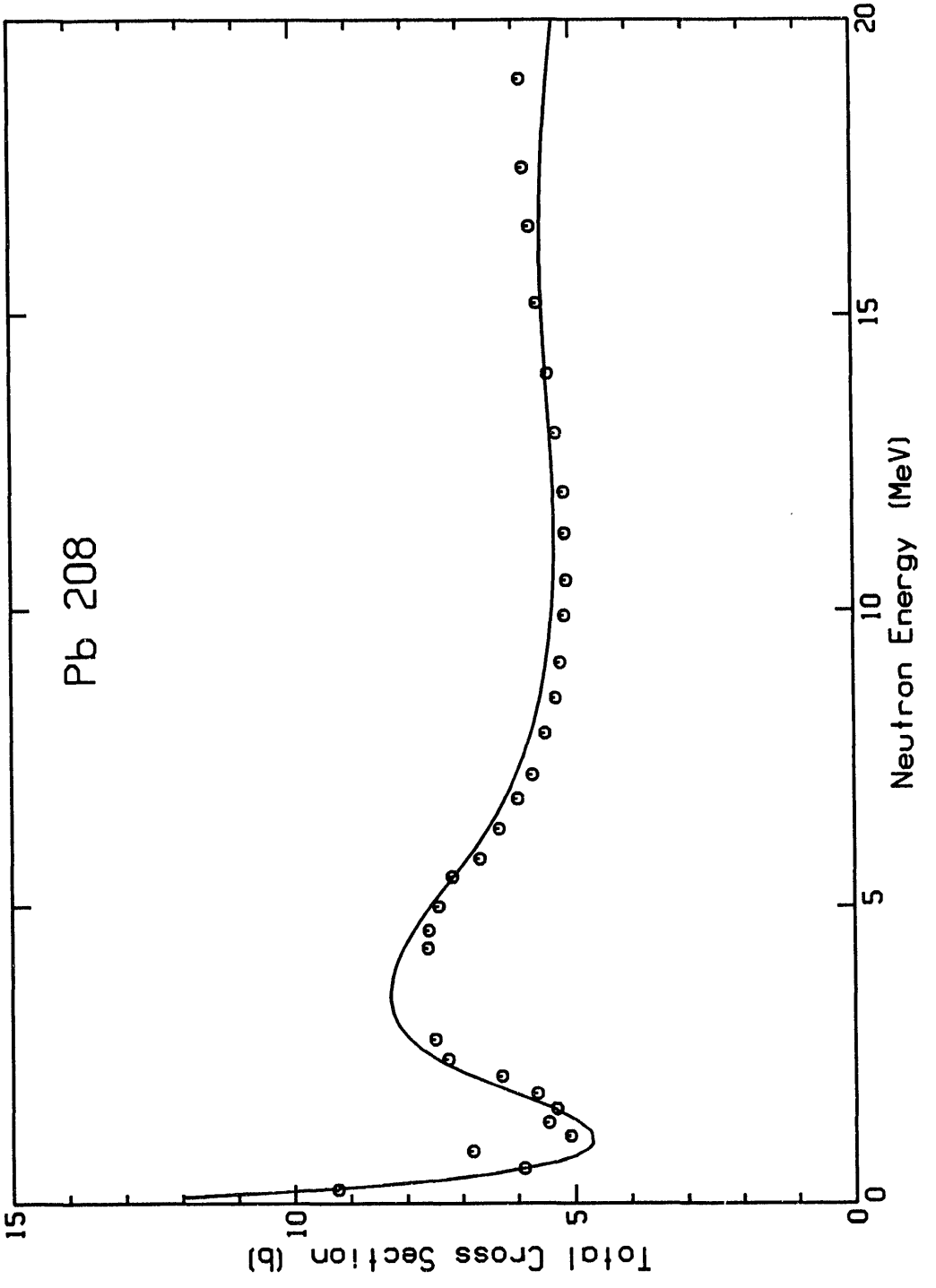


Figure 6

DE-FG05-86ER40293-7

Abstract Submitted

for the Washington, DC Meeting of the

American Physical Society

20-23 Apr. 1992
Date

Physical Review
Analytic Subject Index
Number 25.40.Dn

Sort No.: K.10

Bulletin Subject Heading
in which Paper should be placed
Elastic Neutron Scattering

Neutron Physics

R-matrix analysis of an ORELA measurement of the $n+^{48}Ca$ total cross section from 100 keV to 3.9 MeV.
R. F. CARLTON, Middle Tennessee State Univ. C. H. JOHNSON and J. A. HARVEY, ORNL, — Earlier work[1] predicted little *s*-wave strength in the region above 2 MeV, based on shell model in the continuum calculations. Only three narrow low energy resonances were consistent with a $1/2^+$ assignment. With improved statistics we conclude only one of these is *s*-wave, and have identified a total of 9 below 4-MeV. The strength function based on the earlier work was $\approx 10\%$ of the value expected. The current estimate is $(2.6 \pm 1.3)x10^{-4}$ in good agreement with systematic trends. We have made $J^\pi$ assignments to 15 *p*-wave resonances and 38 *d*-wave resonances. The $d_{5/2}$ interaction continues to dominate with a strength of $(10.7 \pm 1.3)x10^{-4}$. Assuming that the observed reduced neutron widths, $\gamma^2_{J\ell}$, are drawn from Porter-Thomas distributions with population means $<\gamma^2_{J\ell}>$, and are larger than $1/4$ that mean, we estimate that we have missed or spuriously identified $2\text{-}p_{1/2}$, $7\text{-}p_{3/2}$, $8\text{-}d_{3/2}$, and $2\text{-}d_{5/2}$ resonances. The observed level densities can be described using the back-shifted Fermi-gas model with density parameters, $a_c = 3.98 \pm 0.14$ MeV$^{-1}$ and $U_o = 0.24 \pm 0.01$ MeV.

Work supported by USDOE contract DE-FG05-86ER40293 with MTSU.

[1] R.F. Carlton, *et.al.*, Nucl. Phys., **A465**, 274 (1987).

Submitted by

RFCarlton
Signature of APS Member

R.F. Carlton MCA537328
Same name typewritten

Box 65 MTSU
Address
Murfreesboro, TN 37132

Abstract Submitted
for the Southeastern Section Meeting of the
American Physical Society
November 12-14, 1992

Suggested title of session
in which paper should be placed
Elastic Neutron Scattering

Physics and Astronomy
Classification Scheme
Number 25.40.Dn

R-Matrix Analysis of Neutron Total Cross Section Data in the MeV Region. R. F. CARLTON,* MTSU, J. A. HARVEY and C. H. JOHNSON, ORNL.† -- Many complications are associated with the resonance analysis of neutron total cross section data. Even for spin-zero nuclei, making definite spin assignments is difficult above about one MeV for all but the lightest nuclei. Also, resonances outside the analyzed energy region are often crucial to the fits and assignments. Good fits to the data may be obtained with incorrect spin and parity assignments since interference between overlapping multiplets can be complex to decipher. Examples will be shown from measurements on $^{48}Ca$, $^{86}Kr$, and $^{208}Pb$. Techniques and methodologies for extracting $J^{\pi}$-separated level densities, strength functions, scattering functions, and R-functions have been developed from this source of information on the properties of states in the unbound region. These deduced quantities can be connected to models of nuclear structure.

*Work supported by USDOE contract DE-FG05-86ER40293 with Middle Tennessee State University.
†The Oak Ridge National Laboratory is managed by Martin Marietta Energy Systems, Inc. for the U. S. Department of Energy under contract DE-AC05-84OR21400.

RFCarlton
Signature of APS Member

(x) Prefer Standard Session

R. F. Carlton
Middle Tennessee State University
Dept. of Physics & Chemistry
P. O. Box 65
Murfreesboro, TN 37132

DATE
FILMED
7/13/93